Relative Conformational Stabilities of Single-Chain Pocket and Groove-Shaped Antibody Active Sites Including HCDR Transplant Intermediates†

Gene A. Gulliver,‡ Catherine A. Rumbley,§ Jenny Carrero,‡ and Edward W. Voss, Jr.*,‡

Department of Microbiology and Department of Cell and Structural Biology, University of Illinois at Urbana−Champaign, 407 South Goodwin Avenue, Urbana, Illinois 61801

Received November 17, 1994; Revised Manuscript Received February 6, 1995®

ABSTRACT: Stability measurements of SCA 04-01/212 (anti-ssDNA) which possesses a groove-shaped active site were performed by Gdn-HCl-induced unfolding, analyzed assuming a simple two-state equilibrium, and expressed as the free energy of unfolding, ΔG_{n-u}. A ΔG_{n-u} of 1.44 ± 0.13 kcal/mol was determined experimentally for SCA 04-01/212. In addition, the conformational stabilities of HCDR transplants, hybrid antibody molecules resulting from the transplantation of HCDRs from SCA 4-4-20 (anti-fluorescein) into the corresponding regions of 04-01 in all combinations, were determined using the identical protocol applied to SCA 04-01. On the basis of the results of these stability experiments, the HCDR transplants were categorized into three groups, representing low, intermediate, and high stability. Data were discussed in terms of the relationships between structure−function and conformational stability pertaining to the groove-shaped antibody active site of SCA 04-01/212 and the pocket-shaped active site of SCA 4-4-20/212.

Detailed analyses of monoclonal antibodies 4-4-20 (anti-Fl) and 04-01 (autoanti-ssDNA)[1] have provided important insights into structure−function relationships in antibody active sites (Denzin *et al.*, 1991, 1993; Rumbley *et al.*, 1993). X-ray diffraction analyses have demonstrated that the Mab 4-4-20 active site possesses a deep pocket structure which sequesters bound fluorescein, while Mab 04-01 features a relatively shallow cleft, accommodating linear polynucleotides (Herron *et al.*, 1989, 1991). Site-specific mutagenesis analyses have elucidated ligand contact residues critical to wild-type Mab 4-4-20 and 04-01 antibody binding interactions (Denzin *et al.*, 1993; Rumbley *et al.*, 1993). The unique active-site structures and specificities of these two antibodies have previously been suggested to be a function of properties intrinsic to their respective heavy chains (Gulliver *et al.*, 1994; Gulliver & Voss, 1994), since the light chains are nearly identical and the heavy chains differ significantly (Bedzyk *et al.*, 1990a; Smith *et al.*, 1989; Smith & Voss, 1990).

Single-chain antibody (SCA) derivatives of Mab 4-4-20 and 04-01 have been validated as model moleclules for antibody active-site structure−function analyses (Bedzyk *et al.*, 1990b; Denzin *et al.*, 1991; Rumbley *et al.*, 1993). For example, SCA 4-4-20/212, with a 14-amino acid linker (212) tethering V_L to V_H, exhibited a binding affinity for fluorescein within 3−4-fold of Mab 4-4-20, as well as similar Q_{max}, λ_{max}, idiotype, and metatype properties (Bedzyk *et al.*, 1990b; Denzin *et al.*, 1991). Likewise, SCA 04-01/212 demonstrated a binding affinity for p(dT)$_8$ within 3−4-fold of Fab 04-01 (Rumbley *et al.*, 1993). Collectively, these findings suggested that single-chain antibody derivatives of 4-4-20 and 04-01 served as genuine replicas of the native state conformation of the active sites of the parental monclonal antibody molecules in terms of structure and function.

In addition to the verified applications of the SCA system for structure−function analyses, the SCA system had also proven useful in studies involving protein stability (Pantoliano *et al.*, 1991; Müller *et al.*, 1994). Stability measurements of SCA 4-4-20/212 were conducted by Gdn-HCl-induced unfolding and expressed as the free energy of unfolding, ΔG_{n-u} (Pantoliano *et al.*, 1991). On the basis of the close fit of the SCA 4-4-20 experimental unfolding/refolding transition data to two-state behavior, it was concluded that solvent-induced denaturation of SCAs could accurately be analyzed assuming a simple two-state equilibrium, N⇌U. Because SCA 4-4-20/212 and 04-01/212 share identical peptide linkers, the contribution to SCA conformational stability from the covalent linkage of the V_L and V_H domains had the potential to be relatively constant between the two protein molecules. As a result, the ΔG_{n-u} values obtained for both SCAs could provide insight into the nature of the conformational stability between two diverse antibody active-site structures (i.e., a deep pocket versus a shallow cleft). Consequently, stability measurements of SCA 04-01/212 were performed by Gdn-HCl-induced unfolding, analyzed assuming a simple two-state equilibrium, and expressed as the free energy of unfolding, ΔG_{n-u}. In addition, previously studied HCDR transplants (hybrid antibody proteins resulting from transplantation of HCDRs from 4-4-20 into the corresponding regions of 04-01 in all possible combinations) were also characterized in terms of stability using identical experimental and analytical protocols

† This work was supported by a grant from the Biotechnology Research Development Corp., Peoria, IL.

* Address correspondence to this author. Phone: (217) 333-1738. FAX: (217) 244-6697.

‡ Department of Microbiology.

§ Department of Cell and Structural Biology.

® Abstract published in *Advance ACS Abstracts,* April 1, 1995.

[1] Abbreviations: CDR, complementarity determining region; FR, framework region; HCDR1, -2, or -3, a specific heavy-chain CDR progressing from the amino-terminal to the carboxy-terminal end of the variable domain (when a superscript notation is present, it refers to the immunoglobulin from which the CDR was derived); Mab, monoclonal antibody; SCA, single-chain antibody; ssDNA, single-stranded DNA; V_L and V_H, variable region of immunoglobulin light (L) and heavy (H) chains; Gdn-HCl, guanidine hydrochloride; [D], molar concentration of denaturant.

0006-2960/95/0434-5158$09.00/0

applied to SCA 04-01. The results of conformational stability experiments using HCDR transplants were discussed by comparison with previously determined SCA 4-4-20/212 ΔG_{n-u} values (Pantoliano *et al.*, 1991) and experimentally determined 04-01/212 ΔG_{n-u} values presented in this report.

MATERIALS AND METHODS

Strains, Plasmids, and Media. SCA 04-01 is a single-chain derivative of autoantibody BV04-01 (IgG 2b, *k*) and is expressed in *Escherichia coli* strain GX6712 (F⁻galk2 rpsL cI_{857}) (Rumbley *et al.*, 1993). Plasmid pGX8772 was provided by Enzon (NJ). The expression vector is under the control of an O_L/P_R λ promotor. Protein was expressed by a temperature shift from 30 to 42 °C in *E. coli* strain GX6712 (Scandella *et al.*, 1985). All *E. coli* cultures were grown in Luria broth or 2×YT media containing 100 μg/mL ampicillin.

Large-Scale Expression of SCA 04-01 and HCDR Transplants. SCA 04-01 and HCDR transplants were expressed and refolded as previously described for anti-fluorescein SCAs (Denzin *et al.*, 1991). Affinity purification of SCA 04-01 was accomplished using ssDNA−agarose (Rumbley *et al.*, 1993).

Gdn-HCl-Induced Unfolding/Refolding Equilibria. Changes in SCA 04-01 and HCDR transplant intrinsic Trp/Tyr fluorescence emission spectra were measured at various Gdn-HCl concentrations to monitor the unfolding/refolding transition (Pace, 1986). The excitation wavelength was 280 nm, and fluorescence emission spectra were collected in the 280−450 nm region. The unfolding/refolding transitions were monitored using the pronounced bathochromic shifts which occurred in the fluorescence emission maximum (λ_{max}) of SCA 04-01 and all HCDR transplants analyzed as a result of increasing concentrations of Gdn-HCl. Fluorescence spectra were collected using a modified ISS (Champaign, IL) GREG-PC spectrofluorometer at the Laboratory for Fluorescence Dynamics (University of Illinois at Urbana−Champaign). Stock solutions of 8.0 M Gdn-HCl were prepared by dissolution in 150 mM NaCl, 50 mM PO_4, pH 8.0. Gdn-HCl solutions were diluted to the appropriate [D], followed by addition of SCA 04-01 or the appropriate HCDR transplant to a final concentration of 5 μg/mL. Unfolding of SCA 04-01 and various HCDR transplants was accomplished by incubating Gdn-HCl/SCA 04-01 solutions at room temperature for 2 h or longer. Renaturation analysis was accomplished by diluting SCA 04-01 into 6.0 M Gdn-HCl followed by dilution to the desired [D].

Data Analysis of Unfolding/Refolding Transitions. Data collected from the Gdn-HCl-induced denaturation of SCA 04-01 and the various transplants were analyzed by assuming a two-state approximation, N ⇔ U. The latter assumed that the concentration of intermediates along the unfolding/refolding pathway was negligible compared to the concentrations of N and U states. Linear extrapolation was used to estimate conformational stability, ΔG_{n-u}, of the various SCAs. ΔG_{obs} and K_{obs} values were calculated using

$$K_{obs} = e^{-\Delta G/RT} = f_U/f_N = (y - y_N)/(y_U - y) \quad (1)$$

where y_N and y_U were λ_{max} values characteristic of the N and U forms of SCA 04-01, and y is the λ_{max} value at a given concentration of Gdn-HCl. Linear extrapolation assumes that

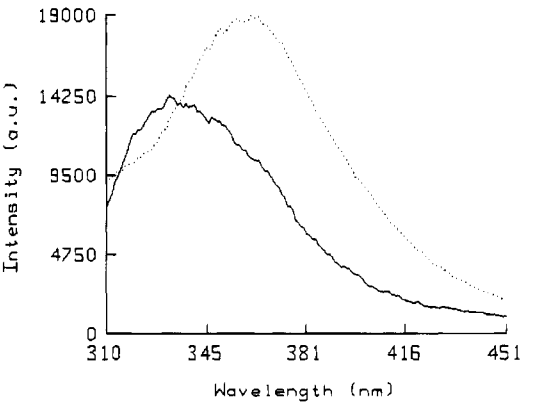

FIGURE 1: Fluorescence spectra of SCA 04-01 at 0 (—) and 5M (•••) Gdn-HCl. Excitation wavelength was 280 nm.

in the transition region of unfolding there is a linear dependence of ΔG_{n-u} on denaturant concentration which can be extrapolated to zero concentration of denaturant. Consequently, data analyzed were fit to the equation:

$$\Delta G_{obs} = \Delta G_{n-u} + m[D] \quad (2)$$

where m is the slope of the linear denaturation plot, and ΔG_{n-u} is the free energy change for unfolding at [D] = 0, or the y-intercept.

$\Delta\Delta G_u$ values were calculated using the equation:

$$\Delta\Delta G_u = \Delta G_{mutant} - \Delta G_{wild\ type} \quad (3)$$

RESULTS

Effects of Gdn-HCl on the Intrinsic Fluorescence of SCA 04-01 and HCDR Transplants. The Trp and Tyr contents of SCA 04-01 were determined as previously described (Smith & Voss, 1990). The V_L and V_H regions contained a combined total of 5 Trp residues and 11 Tyr residues. The effect of [Gdn-HCl] on the Trp environment of SCA 04-01 and HCDR transplants was determined by the fluorescence λ_{max} and the relative fluorescence quantum yield (integrated intensity). As the Gdn-HCl concentration increased from 0 to 5 M, the fluorescence spectra of the Trp/Tyr residues in SCA 04-01 and the various transplant molecules exhibited a significant red shift, as demonstrated by SCA 04-01 in Figure 1.

SCA 04-01 Denaturation Curve Analysis. Extrapolation from the linear portions of the denaturation curve at low and high Gdn-HCl concentrations yielded λ_{max} values characteristic of the native, y_N, and unfolded, y_U, states for SCA 04-01 (Figure 2). The value of y_N = 331.5 nm while y_U = 356.5 nm. These values were combined with values of y in eq 2 at various concentrations of Gdn-HCl in order to determine ΔG_{obs} at a given concentration of denaturant. The C_m = [D] at the midpoint of the unfolding transition and was determined to be ≅1.3 M for the unfolding of SCA 04-01. Identical analyses were applied to the various HCDR transplants to determine ΔG_{obs} values.

Reversibility of Gdn-HCl-Induced Denaturation of SCA 04-01. Figure 3 shows the nearly complete reversibility of SCA 04-01 unfolding. The two curves generated from SCA 04-01 unfolding and refolding seemed to share similar transitions and plateaus at equivalent concentrations of Gdn-HCl (Figure 3).

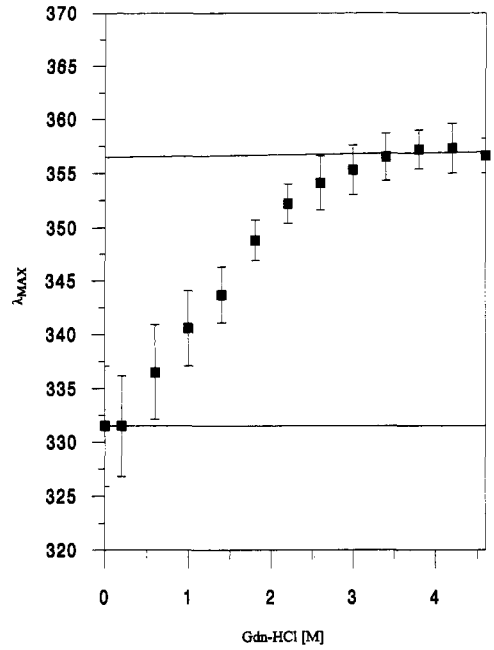

FIGURE 2: Dependence of the fluorescence λ_{max} of SCA 04-01 on Gdn-HCl concentration. Squares indicate the wavelength position of λ_{max} at given concentrations of denaturant. The continuous lines at low and high concentration are the result of linear extrapolation to obtain λ_{max} values characteristic of the native, $y_N = 331.5$, and unfolded, $y_U = 356.5$, states.

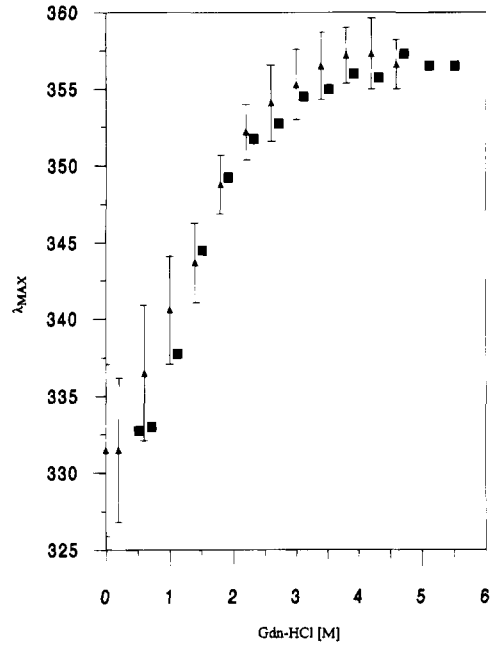

FIGURE 3: Reversibility of SCA 04-01 unfolding. SCA 04-01 was denatured in 6 M Gdn-HCl and diluted to the appropriate concentration of Gdn-HCl (triangles). All reversibility data points represent the results of duplicate trials. The unfolding profile of SCA 04-01 is also shown (squares).

Estimation of ΔG_{n-u} for SCA 04-01 Using Linear Extrapolation. Figure 4 is a plot of the free energies of unfolding versus the concentration of Gdn-HCl. Individual ΔG_{obs} values were calculated using eq 1 and plotted against Gdn-HCl concentration. The ΔG_{n-u} and m from eq 2 were determined by fitting the data to a simple regression equation (a straight line). The ΔG_{n-u} for SCA 04-01 was determined to be 1.5 kcal/mol, while $m \cong 1.08$ kcal/(mol·M). Identical analyses were applied to the various HCDR transplants.

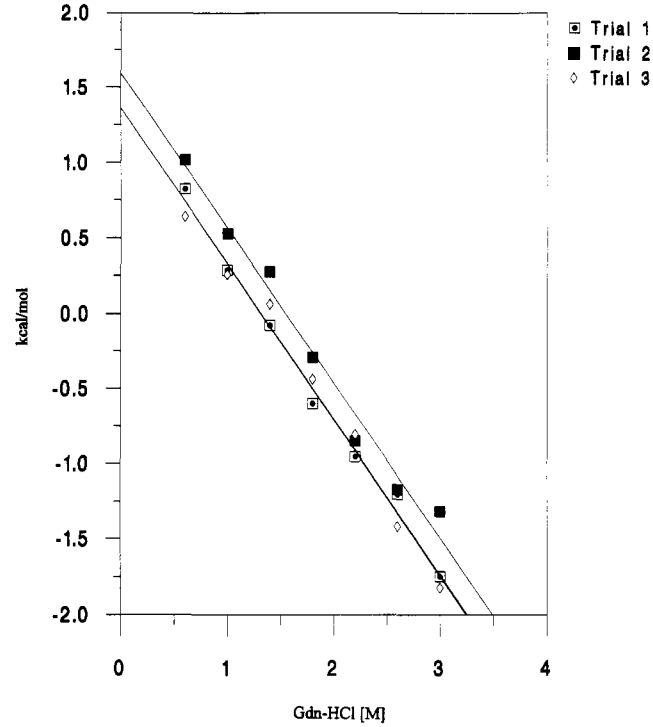

FIGURE 4: ΔG_{obs} as a function of Gdn-HCl concentration for SCA 04-01. The y-intercept represents the approximate ΔG_{n-u} of SCA 04-01, where [Gdn-HCl] = 0 M.

Table 1: Unfolding Properties of SCA 04-01/212 and 4-4-20/(212 or 205c Linker)

SCA/linker	denaturant	$\Delta\lambda_{max}$ (nm)[a]	Δ fluorescence intensity (%)[b]	ΔG_{n-u}[c] kcal/mol
SCA 4-4-20/205c[c]	Gdn-HCl	ND	−40	4.86 ± 0.30
SCA 4-4-20/212[d]	Gdn-HCl	ND	−40	4.33 ± 0.36
SCA 04-01/212	Gdn-HCl	≅25 (red)	+84.93 ± 29.93	1.44 ± 0.13

[a] $\Delta\lambda_{max}$ is the wavelength shift of the fluorescence intensity maximum from 0 to 5 M Gdn-HCl. [b] Δ fluorescence intensity is the change in fluorescence intensity (%) from 0 to 5 M Gdn-HCl. [c] ΔG_{n-u} was calculated as described in the text. Error bars represent standard deviations resulting from three separate experiments. [d] Pantoliano *et al.* (1991).

Unfolding Properties of SCA 04-01/212 and 4-4-20/(212 or 205c Linker). Table 1 demonstrates the differing conformational stability properties of the SCA 04-01 groove-shaped active site relative to the pocket-shaped active site of SCA 4-4-20. C_m's for SCA 4-4-20/212 and 205c (a 25 amino acid linker) were less than that for SCA 04-01/212. However, the calculated conformational stabilities (ΔG_{n-u}) for both SCA 4-4-20 constructs were greater than SCA 04-01 (Table 1).

The fluorescence properties of the unfolding reaction also differed significantly when comparing the SCA 4-4-20 constructs to SCA 04-01 (Table 1). While unfolding of SCA 4-4-20/212 and 205c results in an overall quenching of the intrinsic fluorescence (≅40%) with no apparent shift in the λ_{max}, SCA 04-01 unfolding results in an overall increase in fluorescence intensity (84.93 ± 29.93%) combined with a significant red shift (≅25 nm) in λ_{max}.

Conformational Stabilities of HCDR Transplants. Determination of the free energies of denaturation for the various HCDR transplants suggested that the molecules could be classified into three groups based on relative stability (Table 2). HCDR1-2-3$^{4\text{-}4\text{-}20}$ belonged to group 1 (high stability),

Table 2: Conformational Stabilities of HCDR Transplants[a]

SCA transplant	ΔG_{n-u} (kcal/mol)	$\Delta\Delta G_u$ (relative to 04-01) (kcal/mol)	$\Delta\Delta G_u$[b] (relative to 4-4-20)
HCDR1^{4-4-20}	2.88	1.44	−1.45
HCDR2^{4-4-20}	3.08	1.64	−1.25
HCDR3^{4-4-20}	2.02	0.58	−2.31
HCDR1-2^{4-4-20}	2.87	1.43	−1.46
HCDR1-3^{4-4-20}	2.43	0.99	−1.90
HCDR2-3^{4-4-20}	1.88	0.44	−2.45
HCDR1-2-3^{4-4-20}	3.39	1.95	−0.94

[a] SCA HCDR transplants were constructed and characterized in terms of structure-function as described previously (Gulliver *et al.*, 1994; Gulliver & Voss, 1994). [b] $\Delta\Delta G_u$ was calculated using eq 3.

with a ΔG_{n-u} = 3.39 kcal/mol. HCDR1^{4-4-20}, HCDR2^{4-4-20}, HCDR1-2^{4-4-20}, and HCDR1-3^{4-4-20} were placed in group II (intermediate stability), with ΔG_{n-u} values of 2.88, 3.08, 2.87, and 2.43 kcal/mol, respectively. HCDR3^{4-4-20} and HCDR2-3^{4-4-20}, with ΔG_{n-u} values of 2.02 and 1.88 kcal/mol, respectively, were categorized into group III (low stability).

DISCUSSION

Previous conformational stability analyses of SCA 4-4-20 investigated unfolding/refolding equilibria as a function of Gdn-HCl and urea concentrations. Evidence for intermediate species along the reaction pathway between N and U states was not discovered (Pantoliano *et al.*, 1991). Consequently, it was concluded that a simple two state model, N ⇔ U, had the potential to be applied to the unfolding of SCA 4-4-20, and all other SCA proteins. The simple two-state model, which can apparently be applied to SCAs, offered a distinct advantage over the more complicated thermodynamic models applied to Fabs (Rowe, 1976). Further benefits afforded by protein refolding and stability studies using SCAs include the observation that SCA unfolding transitions are unimolecular and therefore independent of protein concentration, as opposed to the bimolecular protein concentration-dependent unfolding transitions resulting from the noncovalent heterodimer association of Fvs (Pantoliano *et al.*, 1991).

The apparent two-state behavior of SCAs has been argued to depend on the coupling of V_L and V_H domains into a cooperative folding unit, dictated by ΔG_{AB}, the free energy of interdomain association, and ΔG_A and ΔG_B, the free energy of unfolding of individual domains V_H and V_L, respectively (Pantoliano *et al.*, 1991). The contribution of the polylinker to the conformational stability of a SCA has been hypothesized to be due to the entropic effect of covalent linkage between the V_L and V_H domains (Pantoliano *et al.*, 1991), which results in a larger ΔG_{AB} than would be expected for the comparable F_V (Bird *et al.*, 1988). The increased ΔG_{AB} provided by a given polylinker will probably vary, depending on the properties of both the individual polylinker and the covalently attached V_H and V_L domains (Pantoliano *et al.*, 1991). If, however, two SCAs share identical polylinkers, there exists a possibility that the thermodynamic contribution of the polylinker to the conformational stability of a SCA could be normalized. This would enable one to do experiments which concentrate solely on the V_H and V_L inter- and intradomain free energy interactions responsible for the native state conformation of the antibody active site replicated by the SCA. SCA 4-4-20/212 and 04-01/212 allowed the opportunity for such analysis, as they share the same 212 polylinker.

The antibody active sites of 4-4-20 and 04-01 have been extensively characterized in terms of structure−function relationships critical to ligand binding. X-ray crystallography and site-specific mutagenesis analyses have elucidated those amino acid residues within the 4-4-20 and 04-01 antibody active sites which are mandatory for wild-type binding interactions with fluorescein and ssDNA, respectively (Herron *et al.*, 1989, 1991; Denzin *et al.*, 1993; Rumbley *et al.*, 1993). While these studies have provided crucial insight into the biochemical interactions necessary for binding of hapten and polymeric ligands, the V_L and V_H inter- and intrachain protein−protein interactions required to establish an antibody active-site conformation which positions ligand contact residues in an orientation compatible with ligand binding have been difficult to ascertain due to the inherent complexity of the problem. The diverse antibody active-site conformations of 4-4-20 and 04-01, a deep pocket versus a shallow cleft, respectively, have been demonstrated to be advantageous to the study of such problems. For example, primary structural analysis of 4-4-20 and 04-01 revealed nearly identical V_L sequences between the two antibodies, yet differing V_H sequences (Bedzyk *et al.*, 1990a; Smith *et al.*, 1989; Smith & Voss, 1990). These results suggested that the unique active-site conformations of these two antibodies were dictated by properties intrinsic to the heavy chain. Further experimental evidence in support of this hypothesis was provided by HCDR transplantation experiments, in conjunction with *in vivo* heavy- and light-chain reassociation analyses (Gulliver *et al.*, 1994; Gulliver & Voss, 1994).

Results from HCDR transplantation experiments indicated that the formation of an antibody active-site conformation capable of binding polymeric ligands, i.e., DNA, appeared to require less stringent protein−protein interactions between the CDR loops and β-pleated-sheet framework regions than the pocket-shaped antibody active site capable of binding and sequestering a haptenic ligand like fluorescein (4-4-20). While pinpointing the exact biochemical and biophysical properties underlying these complex protein−protein interactions represents a formidable task, a general approximation of the thermodynamic favorability of these cryptic interactions is made possible by an analysis of the overall conformational stabilities of these diverse antibody active sites in the context of the SCA system.

The conformational stability of SCA 4-4-20/212 was previously calculated to have an approximate ΔG_{n-u} = 4.33 kcal/mol (Pantoliano *et al.*, 1991), while for SCA 04-01/212 the ΔG_{n-u} was calculated to be approximately 1.5 kcal/mol. When combined with earlier HCDR transplantation experiments, the results of thermodynamic measurements indicated that while the formation of a pocket-shaped antibody active site required more stringent inter- and intrachain protein−protein interactions between the CDR loops and β-sheet framework regions in the V_L and V_H, these interactions ultimately resulted in an antibody active-site conformation which was more thermodynamically favorable than a groove-shaped antibody active site. The biological significance of such a scenario is appreciated when considering the conformational dynamics which have been hypothesized to occur upon *in vivo* binding of haptenic and polymeric ligands (Miklasz *et al.*, 1994). The conformational dynamics of an autoimmune cross-reactive anti-DNA anti-

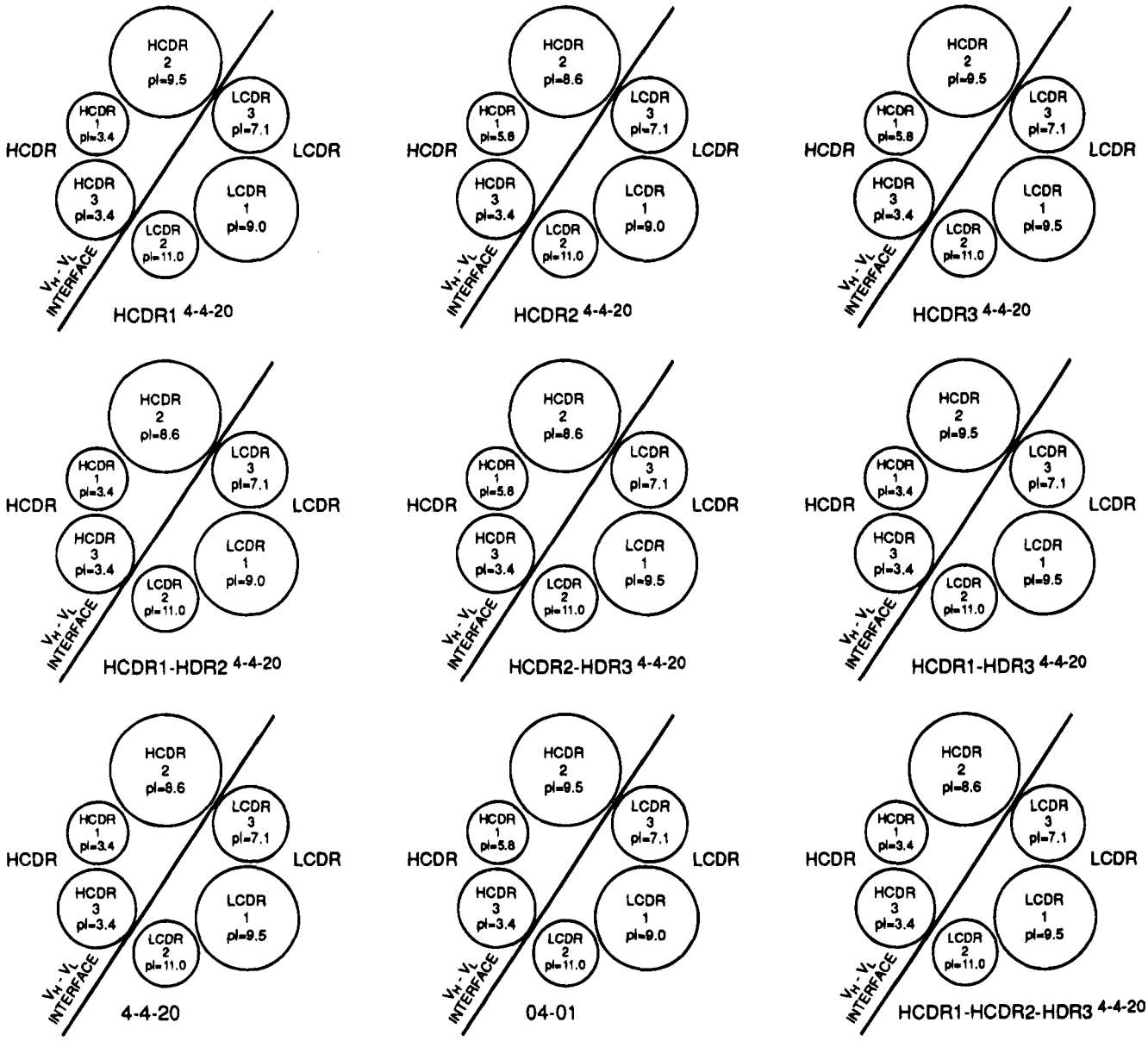

FIGURE 5: Theoretical isoelectric points (p*I*) of the complementarity-determining regions of 04-01, 4-4-20, and the various HCDR transplants. Circles represent individual CDRs. The size of each circle is proportional to the molecular weight of the represented CDR.

body like 04-01 may benefit from an active site with a negligible ΔG_{n-u} in order to bind with low or intermediate affinity to the various DNA moieties encountered *in vivo*, by allowing for a more malleable antibody active-site conformation. Conversely, an antibody like 4-4-20 may require a more thermodynamically stable and conformationally rigid active site in order to consistently present antigenic contact residues in an orientation capable of binding haptenic ligands like fluorescein *in vivo* with high affinity. In short, the implications of the underlying protein−protein interactions which influence the conformation and stability of an antibody active site are finally manifested when considering the activity of the entire antibody molecule *in vivo*.

Finally, there existed a possibility that comparison of the conformational stability of 4-4-20 and 04-01 active sites using the single-chain antibody system was not entirely suitable because the 212 linker may not have equivalent stabilizing effects in the context of diverse antibody active sites, i.e., 4-4-20 vs 04-01 active sites. A solution to this uncertainty could be attained by comparing the conformational stabilities of SCA 4-4-20 and SCA 04-01 in the context of various linkers. The conformational stability of SCA 4-4-20 has been determined with two different linkers (212 and 205c) (Pantoliano *et al.*, 1991), and both ΔG_{n-u} values were significantly greater than the ΔG_{n-u} obtained for SCA 04-01/212. Hence, the conformational stability of SCA 04-01 tethered by a 205c linker should be determined and compared to the ΔG_{n-u} values previously obtained for the other SCA proteins. A SCA 04-01/205c ΔG_{n-u} value less than what was obtained for SCA 4-4-20/212 and 205c would support the conclusions presented in this report. Consequently, future experiments involving antibody active-site conformational stability will focus on wild-type and mutant SCAs exploiting various linkers. Knowledge gained from such studies will broaden our understanding of the complex structure−function−stability relationships existing in an antibody active site.

Theoretical isoelectric points (p*I*) of the complementarity-determining regions of 04-01 and 4-4-20 (Figure 5) suggest that the ligand encounters a very specific chemical

environment before it is accommodated in the active site. The theoretical p*I* values for the CDRs of 04-01 and 4-4-20 can be divided into three pairs: acidic (HCDR1,3), neutral (HCDR2, LCDR3), and basic (LCDR1,2) (Figure 5). Consequently, denaturation studies with HCDR transplants can be discussed in terms of isoelectric points, as well as intra- and interchain interactions between CDRs and framework regions of the antibody active site.

The free energies of denaturation for the different transplants are shown in Table 2. All of the HCDR transplants are more resistant to Gdn-HCl denaturation than wild-type SCA 04-01 and less stable than SCA 4-4-20. The transplants have been classified into three groups based on their stabilities (Table 2). HCDR1-2-$3^{4\text{-}4\text{-}20}$ demonstrated the greatest stability against Gdn-HCl denaturation and was therefore placed in group I (high stability). The increased stability relative to the other transplants may be explained by noting that the three HCDRs of SCA HCDR1-2-$3^{4\text{-}4\text{-}20}$ and 4-4-20 are identical, which may be explained by noting that the structural features of the SCA 4-4-20 CDRs appear to increase the overall conformational stability of the SCA 4-4-20 molecule. Group II (intermediate stability) consists of three transplants (HCDR$1^{4\text{-}4\text{-}20}$, HCDR1−HCDR$2^{4\text{-}4\text{-}20}$, and HCDR1−HCDR$3^{4\text{-}4\text{-}20}$) (Figure 5) which share identical p*I* values for the HCDR1,3 acid pair. The decrease in total pI of the HCDR1,3 acid pair in these transplants compared to SCA 04-01 possibly stabilizes the macromolecules of group II because the acidic pair may better balance the p*I* of the adjacent basic pair (LCDR1 and LCDR2) of the light chain. The decreased stability of HCDR1-$3^{4\text{-}4\text{-}20}$ relative to other members of group II was possibly due to a destabilizing interaction between the HCDR2 of 04-01 and the HCDR1 and HCDR3 of 4-4-20, which may explain why HCDR1-$3^{4\text{-}4\text{-}20}$ did not possess the capacity to bind either Fl or ss-DNA (Gulliver *et al.*, 1994; Gulliver & Voss, 1994). HCDR$2^{4\text{-}4\text{-}20}$ was stabilized with respect to 04-01, potentially because the exchange of HCDR2 04-01 for HCDR2 4-4-20 brings the p*I* of the neutral pair even closer to neutrality. The latter decreases the electrostatic interaction of the acidic pair with the neutral pair and allows the acidic pair to have a stronger intrachain interaction with the basic pair. Finally, the decreased stability of group III transplants may reflect the destabilizing effect of mutating SCA 04-01 HCDR3, the most highly variable region in nearly all antibody active sites due to somatic recombination in the germline genes. As expected, this increased HCDR3 variability is also observed in the case of SCA 04-01 and 4-4-20, which may relate to the differences in stability between both antibody active sites. The HCDR3 region protein−protein interactions (i.e., CDR−CDR, FR−CDR) from 4-4-20 may contribute to the overall increase in stability when present in the proper antibody active-site context, as is the case with SCA 4-4-20. If, however, HCDR3 4-4-20 is placed in an unfavorable antibody active-site environment, the stabilizing effect of HCDR3 4-4-20 is decreased, as was observed with transplants HCDR$3^{4\text{-}4\text{-}20}$, HCDR1−HCDR$3^{4\text{-}4\text{-}20}$, and HCDR2−HCDR$3^{4\text{-}4\text{-}20}$. Hence, in addition to providing a specific chemical environment for ligand binding, the isoelectric points and structural characteristics of the CDRs may also contribute to the overall stability of the unliganded antibody active site.

ACKNOWLEDGMENT

We thank Mark Mummert and Bill Mallender for their valuable insights during the preparation of the manuscript. We also express our gratitude to all members of the Laboratory for Fluorescence Dynamics (University of Illinois, Urbana) for their expert services throughout the course of this study.

REFERENCES

Bedzyk, W. D., Herron, J. N., Edmundson, A. B., & Voss, E. W., Jr. (1990a) *J. Biol. Chem. 265*, 133−138.

Bedzyk, W. D., Weidner, K. M., Denzin, L. K., Johnson, L. S., Hardman, K. D., Pantoliano, M. W., Asel, E. K., & Voss, E. W., Jr. (1990b) *J. Biol. Chem. 265*, 18615−18620.

Bird, R. E., Hardman, K. D., Jacobson, J. W., Johnson, S., Kaukman, B. M., Lee, S. M., Lee, T., Pope, S. H., Riordan, G. S., & Whitlow, M. (1988) *Science 242*, 423−426.

Denzin, L. K., Whitlow, M., & Voss, E. W., Jr. (1991) *J. Biol. Chem. 266*, 14095−14103.

Denzin, L. K., Gulliver, G. A., & Voss, E. W., Jr. (1993) *Mol. Immunol. 30*, 1331−1345.

Gulliver, G. A., & Voss, E. W., Jr. (1994) *J. Biol. Chem. 269*, 24040−24045.

Gulliver, G. A., Bedzyk, W. D., Smith, R. G., Bode, S. L., Tetin, S. Y., & Voss, E. W., Jr. (1994) *J. Biol. Chem. 269*, 7934−7940.

Herron, J. N., He, X., Mason, M. L., Voss, E. W., Jr., & Edmundson, A. B. (1989) *Proteins: Struct., Funct., Genet. 5*, 271−280.

Herron, J. N., He, X. M., Ballard, D. W., Blier, P. R., Pace, P. E., Bothwell, A., Voss E. W., Jr., & Edmundson, A. B. (1991) *Proteins: Struct., Funct., Genet. 11*, 159−175.

Miklasz, S. D., Gulliver, G. A., & Voss, E. W., Jr. (1994) *J. Mol. Recognit.* (submitted for publication).

Müller, J. D., Nienhaus, G. U., Tetin, S. Y., & Voss, E. W., Jr. (1994) *Biochemistry 33*, 6221−6227.

Pace, C. N. (1986) *Methods Enzymol. 131*, 266−280.

Pantoliano, M. W., Bird, R. E., Johnson, S., Asel, E. D., Dodd, S. W., Wood, J. F., & Hardman, K. D. (1991) *Biochemistry 30*, 10117−10125.

Rowe, E. S. (1976) *Biochemistry 15*, 905−916.

Rumbley, C. A., Denzin, L. K., Yantz, L., Tetin, S. Y., & Voss, E. W., Jr. (1993) *J. Biol. Chem. 268*, 13667−13674.

Scandella, D., Arther. P., Mattingly, M., & Neuhold, L. (1985) *J. Biol. Chem. 9B*, 203.

Smith, R. G., Ballard, D. W., Blier, P. R., Pace, P. E., Bothwell, A., Herron, J. N., Edmundson, A. B., & Voss, E. W., Jr. (1989) *J. Indian. Inst. Sci. 69*, 25−46.

Smith, R. S., & Voss, E. W., Jr. (1990) *Mol. Immunol. 27*, 463−470.

BI9426726